

## A novel approach of fMRI-guided tractography analysis within a group: construction of an fMRI-guided tractographic atlas

Maria Giulia Preti, Nikos Makris, Maria Marcella Laganà, George Papadimitriou, Francesca Baglio, Ludovica Griffanti, Raffaello Nemni, Pietro Cecconi, Carl-Fredrik Westin and Giuseppe Baselli

**Abstract**— Diffusion Tensor Imaging (DTI) tractography and functional Magnetic Resonance Imaging (fMRI) investigate two complementary aspects of brain networks: white matter (WM) anatomical connectivity and gray matter (GM) function. However, integration standards have yet to be defined; namely, individual fMRI-driven tractography is usually applied and only few studies address group analysis. This work proposes an efficient method of fMRI-driven tractography at group level through the creation of a tractographic atlas starting from the GM areas activated by a verbal fluency task in 11 healthy subjects. The individual tracts were registered to the MNI space. Selection ROIs derived by GM masking and dilation of group activated areas were applied to obtain the fMRI-driven subsets within tracts. An atlas of the tracts recruited among the population was obtained by selecting for each subject the fMRI-guided tracts passing through the high probability voxels (the voxels recruited by the 90% of the subjects) and merging them together. The reliability of this approach was assessed by comparing it with the probabilistic atlas previously introduced in literature. The introduced method allowed to successfully reconstruct activated tracts, which comprehended corpus callosum, left cingulum and arcuate, a small portion of the right arcuate, both cortico-spinal tracts and inferior fronto-occipital fasciculi. Moreover, it proved to give results concordant with the previously introduced probabilistic approach, allowing in addition to reconstruct 3D trajectories of the activated fibers, which appear particularly helpful in the detection of WM connections.

### I. INTRODUCTION

White matter (WM) tractography based on Diffusion Tensor Imaging (DTI) from Magnetic Resonance Imaging (MRI) represents a powerful non-invasive tool for exploring white matter (WM) tracts in-vivo [1] and

M. G. Preti is with the Dipartimento di Bioingegneria, Politecnico di Milano, Milano, Italy and also with the Fondazione Don Carlo Gnocchi, Milano, Italy. (corresponding author to provide phone: 0039 347 5117107; fax: 02 40308346; e-mail: gpreti@dongnocchi.it).

N. Makris and G. Papadimitriou are with the Harvard Medical School Departments of Neurology and Radiology Services, Center for Morphometric Analysis, A. Martinos Center for Biomedical Imaging, Massachusetts General Hospital, Boston.

N. Makris is also with the Harvard Medical School Department of Psychiatry, Psychiatry Neuroimaging Laboratory, Brigham and Women's Hospital, Boston, and with the Boston University School of Medicine, Department of Anatomy and Neurobiology, Boston.

M. M. Laganà, F. Baglio, L. Griffanti, R. Nemni, P. Cecconi are with the Fondazione Don Carlo Gnocchi, Milano, Italy.

R. Nemni is also with the Università degli Studi di Milano, Milano, Italy.

C. F. Westin is with the Department of Radiology, Brigham and Women's Hospital and Harvard Medical School, Boston.

G. Baselli is with the Dipartimento di Bioingegneria, Politecnico di Milano, Milano, Italy.

investigating the main anatomical features of brain connectivity. Conversely, functional MRI (fMRI) provides information concerning the localization of cortical activations; hence, integration of the two pieces of information in specific brain circuits is gaining increasing attention for a further insight into the correlation between the structure of connectivity and functional response, as well as its damage in neuro-degenerative pathologies and after brain lesions [2]. Several previous studies analyze fMRI and DTI separately [3]-[7]. Recently, some works have integrated the two techniques [8]-[14] focusing on the set of fibers stemming from WM close to fMRI activated areas, either in broad sense or within specific tracts. The explored applications of fMRI-driven tractography are several, such as multiple sclerosis [9] or brain tumors [10], and more can be foreseen, such as neuro-degenerative diseases. Both a functional loss of normal connections (related or not to physical damage) and the recruitment of new ones due to plastic adaptation can be addressed. fMRI-driven techniques, however, still presents open choices in several processing steps; e.g., the choice of the stereotactic space for the registration to be applied in order to combine the activation regions and the tracts, or the definition of the seeding regions for tractography. Several previous studies register the activation regions to the diffusion or structural space of the individual [8], [10], [13], [15]; however, inclusion errors into activation areas due to registration is poorly controlled. A solution is to manually draw the fMRI activation ROIs in the diffusion space [12], though with a strongly operator-dependent procedure.

Further, most of literature studies limit the analysis to the single subject space, and only a few explore the connections at group level [9], [14]. A group-level analysis could consist in the creation of an atlas of the WM tracts recruited during a precise task among a specific population. This would make possible to compare the different recruitment of tracts in different subject samples, for example between healthy subjects and patients. Bonzano et al. [9] processed the individual fMRI-driven tracts to build a probabilistic map of the connections in the analyzed population. However, to our knowledge, no work in literature focuses on the construction of a 3D tractographic atlas. This could be particularly helpful for connectivity detection purposes, for example in order to assess the WM connections between the gray matter (GM) Broadmann areas, which could be shown in three dimensions together with the tracts.

This work aims at suggesting an efficient method of

fMRI-driven tractography at group level, leading to the creation of a tractographic atlas of the connections underlying a specific functional activation within a group of subjects.

## II. METHODS

### A. Subjects

MR images were acquired from 11 Healthy Subjects (HS). These were preliminarily screened to exclude major systemic, psychiatric or neurological illnesses. The study was conformed to the ethical principles of the Helsinki Declaration and informed written consent was obtained from all subjects.

### B. MRI Acquisitions

Brain MRI acquisitions were performed using a 1.5 Tesla scanner (Siemens Magnetom Avanto, Erlangen, Germany), including the following sequences: 1) 3-dimensional T1-weighted magnetization prepared rapid gradient echo (MPRAGE) (TR = 1,900 ms, TE = 3.37 ms, TI = 1,100 ms, flip angle = 15°, 176 contiguous, axial slices with voxel size = 1 mm × 1 mm × 1 mm, matrix size = 192 × 256, FOV = 192 × 256 mm, and slab thickness = 176 mm) used as anatomical scan for fMRI analysis.; 2) diffusion weighted (DW) pulsed-gradient spin-echo planar (TR=7000 ms, TE=94 ms, 50 2.5-mm-thick axial slices, matrix size=128×96, FOV=320mm × 240 mm), with diffusion gradients (b-value=900s/mm<sup>2</sup>) applied in 12 non-collinear directions. Two runs of images were acquired for each HS, with one b=0 image without diffusion weighting; 3) single-shot gradient echo EPI sequence (TR/TE = 3000/50ms, FOV = 250mm, matrix size = 64×64, in-plane resolution = 3.9 × 3.9 mm<sup>2</sup>) using blood oxygenation level dependent (BOLD) contrast for functional imaging, acquired with a verbal fluency task. Each session included 120 volumes consisting of 38 axial slices with a 3mm thickness in order to cover the entire brain.

### C. DTI Analysis

DWI data were corrected for eddy current distortions and the two runs were registered to the same space for each HS using FSL (FMRIB's Software Library, www.fmrib.ox.ac.uk/fsl), by estimating the transformation between the b=0 image of the second run and the b=0 image of the first one and by applying it to all the DWI of the second run. The DT was estimated with Diffusion Toolkit (www.trackvis.org) v0.6, which firstly rotates the B-matrix for slice angulation and for the rotation applied. Tractography was performed with Diffusion Toolkit, using the brute force approach and the Interpolated Streamline deterministic algorithm. Conventional thresholds of angle=35° and a Fractional Anisotropy (FA)=0.2 were adopted as stopping criteria.

### D. fMRI Analysis

fMRI data processing was carried out using FEAT Version 5.98, part of FSL, with the default parameters suggested by FSL and reported hereon. Prestatistic processing included motion correction using FLIRT, non brain structures removal using BET, spatial smoothing with a Gaussian kernel of 5 mm and high pass filtering with a cutoff of 60s. FILM was used to perform the time-series statistical analysis with local autocorrelation correction and motion parameters were included in the model as regressors. Z statistics images were thresholded using clusters determined by  $Z > 2.3$  and a corrected cluster significance threshold of  $P = 0.05$ . The second-level analysis was carried out with FSL to assess the group average activations. Registration to high-resolution structural images (T1-mprage) was carried out using FLIRT. Registration from high resolution structural to standard space was then further refined using FNIRT nonlinear registration.

### E. fMRI-guided tractography

In order to be able to combine data from fMRI and DTI, we registered the tracts of each HS to the MNI space, in which the fMRI group activation maps are. The linear transformation between the FA map of each HS and the template FA in MNI coordinates (FMRIB58\_FA) was estimated using FLIRT and applied to the brain tracts using TrackVis. The activation regions of the group average Z image resulting from the second level fMRI analysis were first masked with a GM template in MNI coordinates and then dilated to reach the WM using a spherical kernel of 3mm. Then, the obtained activation ROIs were imported in TrackVis (www.trackvis.org) and for every HS only the tracts passing through these ROIs were selected. We will refer to these tracts as to *activated tracts*. Starting from the activated tracts of every HS, we proceeded in two steps to create the fMRI-driven tractographic atlas:

#### 1) fMRI-guided probabilistic map:

The density maps of the activated tracts for every individual, which are already in MNI standard coordinates, were created using TrackVis and binarised. All binary maps were then averaged, in order to obtain a probabilistic map of the activated bundles in the group [9].

#### 2) fMRI-guided tractographic atlas:

The previously created probabilistic map was thresholded at a value of 0.9, in order to highlight the high probability voxels among the observed population. Then, for every HS only the activated tracts passing through the high probability regions were selected and merged together, in order to obtain a tractographic template of the activated tracts in the healthy condition.

### F. Comparison between tractographic and probabilistic atlas

The obtained fMRI-guided tractographic atlas was compared with the probabilistic approach introduced by Bonzano [9],

to assess the concordance of their results. To perform a comparison, a density map of the fMRI-guided tractographic atlas was created and the number of overlapping voxels between this image and the fMRI-guided probabilistic map thresholded at a value of 0.1 to exclude only the less probable voxels was assessed. Two percentages of overlap were then computed: the former as the percentage of overlapping voxels normalized by the number of voxels of the probabilistic map, the latter as the percentage of overlapping voxels normalized by the number of voxels of the tractographic atlas.

### III. RESULTS

The Z-statistics image resulting from the second level fMRI analysis is shown in Fig. 1. Significant activations were found mostly in the left hemisphere as well as in the cerebellum. In Fig. 2, the fMRI-guided probabilistic map is observable. Fig. 3 shows instead the fMRI-guided tractographic atlas, given by the merging of the individual tracts passing through the high probability regions. A large portion of WM bundles resulted to be involved in the considered task, comprehending corpus callosum, left cingulum and arcuate fasciculus, a small portion of the right arcuate fasciculus, right and left cortico-spinal tracts and inferior fronto-occipital fasciculi. The voxels found to be overlapping between the two methods corresponded to a percentage of the 79% of the voxels of the probabilistic atlas, and the 71% of the voxels of the tractographic atlas.

### IV. DISCUSSION

The present study aimed at introducing an efficient and operator-independent method of fMRI-guided tractography analysis at group level. An fMRI-driven tractographic atlas was constructed in order to investigate the WM connections underlying a specific functional activation, among a group of subjects. This group-level analysis appears particularly useful for future studies on patients, when there is an interest in assessing the differences between the pathological and the normal condition in the recruitment of tracts for a specific functional task. In the presence of WM or GM damages, in fact, a loss of connectivity or the recruitment of new circuits due to plasticity could be found. In addition, our particular aim was to obtain an atlas of 3D trajectories (different from a probabilistic image) allowing us to investigate the anatomical connectivity between WM and/or GM regions. Therefore, the constructed fMRI-guided tractographic atlas comprehends actual fibers that can be inspected in 3-dimensional space. GM/WM template regions in MNI coordinates can be over-imposed to the atlas tracts, allowing the direct visual investigation of the anatomical WM connections. Moreover, the 3D tract reconstruction allows an easier classification of the different WM bundles recruited. To construct the tractographic atlas, we used a previously reconstructed probabilistic map of the fMRI-guided tracts, in order to select and merge only those tracts that pass through the high probability voxels. 0.9 was chosen as threshold for

the probabilistic map in order to highlight the voxels with almost certainty of belonging to the activated tracts. By introducing a tractographic atlas, we included in the observation also voxels which are in "low probability regions" but belong to tracts contributing to form the high probability spots, as these voxels are considered important as well to detect a connection between different brain regions. Certain WM connections could present, in fact, high variability among subjects (causing low probability in the probabilistic map), in particular for patients, but appear anyway important for the detection of connectivity.

The introduced fMRI-guided tractographic atlas allowed to successfully reconstruct 3D trajectories of the WM connections and appeared to be in concordance (overlapping voxels are the 79% and 71% of the probabilistic and tractographic atlas voxels respectively) with the results of the probabilistic atlas introduced in [16] and applied in [9] to the fMRI-guided tractography analysis. The two approaches lead to conceptually different results (a probability map in one case, a 3D bundle in the other one) and the choice between them could depend on one's particular need. As already mentioned, the main aim of the tractographic atlas is to provide 3D tracts useful to detect the WM connections between different WM and/or GM areas, whereas the fMRI-guided probabilistic map appears particularly useful in quantitative studies. For example, it allows to weigh the diffusion indices computed along a bundle (e.g. FA, Mean Diffusivity, Axial and Radial Diffusivity) for the probability of one WM voxel to be activated.

As regards the choice of the stereotactic space in which to combine the DTI and fMRI data, we transformed the brain tracts to the MNI standard space, allowing therefore to directly combine the activations (which are already in MNI coordinates) with the diffusion data without applying any transformation to the former. Moreover, as the normalisation of tracts was performed after their generation in the subject's native space, this method does not require to deal with tensor registration and reorientation. As to the definition of the selection ROIs for tractography, the activation regions were first masked with a GM template in MNI coordinates in order to avoid the inclusion of voxels outside the GM, due to fMRI or registration artefacts. Then, the activation ROIs were dilated in order to include WM/GM interface and be able to initiate tractography: we chose to be as conservative as possible, adopting the smallest dilation (3mm), which allowed WM tract reconstruction.

Future developments of this work will consist in the inclusion of more HS in the atlas and in the application of the same approach to patients affected by WM or GM damages. The limited number of HS, in fact, is a weakness of this study and the future enlargement of the sample is necessary to confirm the results. Further, the application to patients will allow to assess the different behaviour of HS and patients, and to investigate the possible recruitment in patients of compensation circuits allowing them to preserve a good functionality of the brain.

## V. CONCLUSIONS

In this preliminary study, we introduced a method of fMRI-guided tractography group analysis, by constructing an fMRI-guided tractographic atlas of the WM tracts underlying a specific functional activation. We experimented and showed the reliability of the proposed method on a population of 11 HS with a verbal fluency task. Future developments would be required to show the possible applicability of the method to clinical studies aiming at evaluating the changes in the anatomical and functional connectivity on groups of patients.

## REFERENCES

- [1] D. Le Bihan, "Looking into the functional architecture of the brain with diffusion MRI," *Nat. Rev. Neurosci.*, vol. 4, pp. 469-480, Jun. 2003.
- [2] M. Jackowski, C. Y. Kao, M. Qiu, R. T. Constable and L. H. Staib, "White matter tractography by anisotropic wavefront evolution and diffusion tensor imaging," *Med. Image Anal.*, vol. 9, pp. 427-440, Oct. 2005.
- [3] R. E. Propper, L. J. O'Donnell, S. Whalen, Y. Tie, I. H. Norton, R. O. Suarez, L. Zollei, A. Radmanesh and A. J. Golby, "A combined fMRI and DTI examination of functional language lateralization and arcuate fasciculus structure: Effects of degree versus direction of hand preference," *Brain Cogn.*, vol. 73, pp. 85-92, Jul. 2010.
- [4] R. G. Schlosser, I. Nenadic, G. Wagner, D. Gullmar, K. von Consbruch, S. Kohler, C. C. Schultz, K. Koch, C. Fitzek, P. M. Matthews, J. R. Reichenbach and H. Sauer, "White matter abnormalities and brain activation in schizophrenia: a combined DTI and fMRI study," *Schizophr. Res.*, vol. 89, pp. 1-11, Jan. 2007.
- [5] S. Aslan, H. Huang, J. Uh, V. Mishra, G. Xiao, M. J. van Osch and H. Lu, "White matter cerebral blood flow is inversely correlated with structural and functional connectivity in the human brain," *Neuroimage*, vol. 56, pp. 1145-1153, Jun. 2011.
- [6] D. J. Werring, C. A. Clark, G. J. Barker, D. H. Miller, G. J. Parker, M. J. Brammer, E. T. Bullmore, V. P. Giampietro and A. J. Thompson, "The structural and functional mechanisms of motor recovery: complementary use of diffusion tensor and functional magnetic resonance imaging in a traumatic injury of the internal capsule," *J. Neurol. Neurosurg. Psychiatry*, vol. 65, pp. 863-869, Dec. 1998.
- [7] K. Zhang, B. Johnson, D. Pennell, W. Ray, W. Sebastianelli and S. Slobounov, "Are functional deficits in concussed individuals consistent with white matter structural alterations: combined FMRI & DTI study," *Exp. Brain Res.*, vol. 204, pp. 57-70, Jul. 2010.
- [8] E. L. Mazerolle, S. D. Beyea, J. R. Gawryluk, K. D. Brewer, C. V. Bowen and R. C. D'Arcy, "Confirming white matter fMRI activation in the corpus callosum: co-localization with DTI tractography," *Neuroimage*, vol. 50, pp. 616-621, Apr. 2010.
- [9] L. Bonzano, M. Pardini, G. L. Mancardi, M. Pizzorno and L. Roccatagliata, "Structural connectivity influences brain activation during PVSAT in Multiple Sclerosis," *Neuroimage*, vol. 44, pp. 9-15, Jan. 2009.
- [10] R. Kleiser, P. Staempfli, A. Valavanis, P. Boesiger and S. Kollias, "Impact of fMRI-guided advanced DTI fiber tracking techniques on their clinical applications in patients with brain tumors," *Neuroradiology*, vol. 52, pp. 37-46, Jan. 2010.
- [11] P. Staempfli, C. Reischauer, T. Jaermann, A. Valvanis, S. Kollias and P. Boesiger, "Combining fMRI and DTI: a framework for exploring the limits of fMRI-guided DTI fiber tracking and for verifying DTI-based fiber tractography results," *Neuroimage*, vol. 39, pp. 119-126, Jan. 2008.
- [12] M. Smits, M. W. Vernooij, P. A. Wielopolski, A. J. Vincent, G. C. Houston and A. van der Lugt, "Incorporating functional MR imaging into diffusion tensor tractography in the preoperative assessment of the corticospinal tract in patients with brain tumors," *AJNR Am. J. Neuroradiol.*, vol. 28, pp. 1354-1361, Aug. 2007.
- [13] M. Ystad, E. Hodneland, S. Adolfsdottir, J. Haasz, A. J. Lundervold, T. Eichele and A. Lundervold, "Cortico-striatal connectivity and cognition in normal aging: a combined DTI and resting state fMRI study," *Neuroimage*, vol. 55, pp. 24-31, Mar. 2011.
- [14] V. L. Morgan, A. Mishra, A. T. Newton, J. C. Gore and Z. Ding, "Integrating functional and diffusion magnetic resonance imaging for

analysis of structure-function relationship in the human language network," *PLoS One*, vol. 4, pp. e6660, Aug. 2009.

[15] A. Venkataraman, Y. Rathi, M. Kubicki, C.-F. Westin and Polina Golland, "Joint Modeling of Anatomical and Functional Connectivity for Population Studies," *IEEE Transactions On Medical Imaging*, vol. 31(2), pp. 164-182, Feb. 2012.

[16] K. Hua, J. Zhang, S. Wakana, H. Jiang, X. Li, D. S. Reich, P. A. Calabresi, J. J. Pekar, P. C. van Zijl and S. Mori, "Tract probability maps in stereotaxic spaces: analyses of white matter anatomy and tract-specific quantification," *Neuroimage*, vol. 39, pp. 336-347, Jan. 2008.

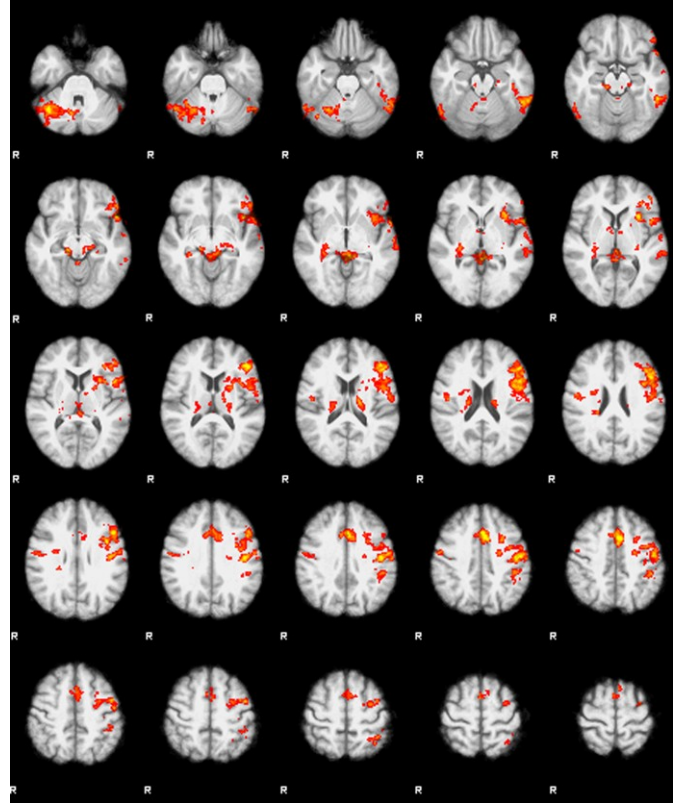


Fig. 1. Z statistics image result from the second level fMRI analysis for the group of 11 healthy subjects.

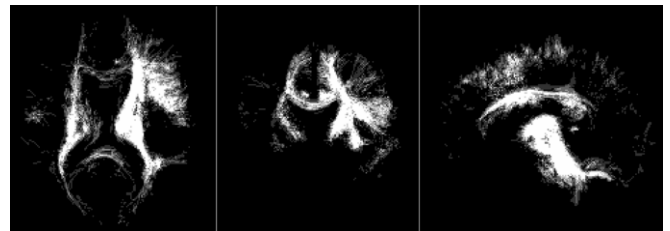


Fig. 2. fMRI-guided probabilistic atlas: map of the probability to belong to the tracts "activated" from the task (not thresholded).

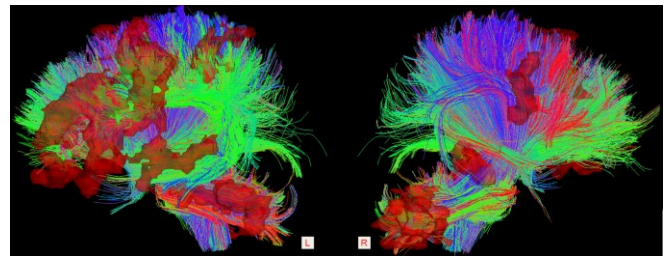


Fig. 3. fMRI-guided tractographic atlas: merging of all subjects' activated tracts passing through high probability regions. The activation ROIs are shown over the tracts.